# High energy photon-neutrino elastic scattering

Ali Abbasabadi
*Department of Physical Sciences, Ferris State University, Big Rapids, Michigan 49307*

Alberto Devoto
*Dipartmento di Fisica, Universitá di Cagliari and INFN, Sezione di Cagliari, Cagliari, Italy*

Wayne W. Repko
*Department of Physics and Astronomy, Michigan State University, East Lansing, Michigan 48824*
(Received 22 December 2000; published 30 March 2001)

The one-loop helicity amplitudes for the elastic scattering process $\gamma\nu\to\gamma\nu$ in the standard model are computed at high center-of-mass energies. A general decomposition of the amplitudes is utilized to investigate the validity of some of the key features of our results. In the center of mass, where $\sqrt{s}=2\omega$, the cross section grows roughly as $\omega^6$ to near the threshold for *W*-boson production, $\sqrt{s}=m_W$. Although suppressed at low energies, we find that the elastic cross section exceeds the cross section for $\gamma\nu\to\gamma\gamma\nu$ when $\sqrt{s}>13\,\mathrm{GeV}$. We demonstrate that the scattered photons are circularly polarized and the net value of the polarization is nonzero. Astrophysical implications of high energy photon-neutrino scattering are discussed.

DOI: 10.1103/PhysRevD.63.093001 PACS number(s): 13.15.+g, 14.60.Lm, 14.70.Bh, 95.30.Cq

## I. INTRODUCTION

The scattering process $\gamma\nu\to\gamma\nu$ has been studied in the past using the four-Fermi theory [1], vector boson theories [2,3], the standard model [4,5], and model-independent parametrizations [6]. At low energies, $\omega\ll m_e$, where $\omega$ is the energy of the photon in the center of mass and $m_e$ is the mass of the electron, the cross section for the elastic scattering $\gamma\nu\to\gamma\nu$ is exceedingly small [5]. As it is shown in the Ref. [7], the cross section for the inelastic process $\gamma\nu\to\gamma\gamma\nu$ is much larger than that of the elastic scattering $\gamma\nu\to\gamma\nu$. However, with increasing $\omega$, the elastic cross section eventually exceeds the inelastic cross section. Here, we show that the crossover occurs at $\omega\sim 7$ GeV.

Our explicit calculations, performed for high energies with massless electron neutrinos, show that the scale for $\gamma\nu\to\gamma\nu$ scattering is set by $m_W$. In fact, the cross section is effectively independent of the electron mass, $m_e$ (except near forward and backward directions). Furthermore, since the weak interaction violates parity, we find a large circular polarization of the scattered photons.

In the next section, we utilize a decomposition of the elastic amplitude $\mathcal{A}(s,t,u)$ to obtain the general properties of and restrictions on the helicity amplitudes $\mathcal{A}_{\lambda_1\lambda_2}(s,t,u)$. Section III contains the numerical results for the complete one-loop helicity dependent differential and total cross sections. This is followed by a discussion of the production of circularly polarized photons in high energy $\gamma\nu\to\gamma\nu$ collisions, and an estimate of the temperature at which, during the thermal evolution of the universe, photons and neutrinos decoupled.

## II. THE $\gamma\nu\to\gamma\nu$ ELASTIC AMPLITUDE

The Lorentz-invariant amplitude for the process $\gamma\nu\to\gamma\nu$ can be expressed as [8]

$$\mathcal{A}(s,t,u)=\overline{u}(p_2)\gamma_\mu(1+\gamma_5)u(p_1)\mathcal{M}_{\mu\alpha\beta}(\varepsilon_1)_\alpha(\varepsilon_2^*)_\beta, \tag{2.1}$$

where $\varepsilon_1$ and $\varepsilon_2^*$ are the polarization vectors for the incoming and outgoing photons, respectively, and the Mandelstam variables $s$, $t$, and $u$ are defined by $s=-(p_1+k_1)^2$, $t=-(p_1-p_2)^2$, and $u=-(p_1-k_2)^2$. Here, the four-momenta of the incoming neutrino and photon are $p_1$ and $k_1$, respectively, with $p_2$ and $k_2$ denoting the corresponding outgoing momenta. The tensor $\mathcal{M}_{\mu\alpha\beta}$ can be expressed in terms of four linearly independent, gauge invariant tensors $T^{(i)}_{\mu\alpha\beta}$, $i=1,...,4$ [8,9]

$$\mathcal{M}_{\mu\alpha\beta}=\mathcal{M}_1(s,t,u)T^{(1)}_{\mu\alpha\beta}+\mathcal{M}_2(s,t,u)T^{(2)}_{\mu\alpha\beta}+\mathcal{M}_3(s,t,u)T^{(3)}_{\mu\alpha\beta}+\mathcal{M}_4(s,t,u)T^{(4)}_{\mu\alpha\beta}. \tag{2.2}$$

To facilitate the inclusion of the Bose symmetry, which requires the invariance of the amplitude under the exchange of the incoming and outgoing photons, we use four tensors $T^{(i)}_{\mu\alpha\beta}$ which have a definite symmetry under this exchange. For our choice, $T^{(1)}_{\mu\alpha\beta}$ is symmetric, while $T^{(2)}_{\mu\alpha\beta}$, $T^{(3)}_{\mu\alpha\beta}$, and $T^{(4)}_{\mu\alpha\beta}$ are antisymmetric. As a consequence, Bose symmetry requires the following relations between the four scalar functions $\mathcal{M}_i(s,t,u)$, $i=1,...,4$:

$$\mathcal{M}_1(s,t,u)=\mathcal{M}_1(u,t,s), \tag{2.3}$$

$$\mathcal{M}_j(s,t,u)=-\mathcal{M}_j(u,t,s),\quad j=2,3,4. \tag{2.4}$$

In the center-of-mass with massless neutrinos, the contractions of the tensors $T^{(i)}_{\mu\alpha\beta}$ with the neutrino factor $\xi_\mu=\overline{u}(p_2)\gamma_\mu(1+\gamma_5)u(p_1)$ and polarization vectors $(\varepsilon_1)_\alpha$ and $(\varepsilon_2^*)_\beta$, result in the following helicity basis [8]:

 

$$T^{(1)}_{\mu\alpha\beta}\xi_\mu(\varepsilon_1)_\alpha(\varepsilon_2^*)_\beta = -s\cos(\theta/2)[t(\lambda_1+\lambda_2+2\lambda_1\lambda_2) + 4s\lambda_1\lambda_2], \tag{2.5}$$

$$T^{(2)}_{\mu\alpha\beta}\xi_\mu(\varepsilon_1)_\alpha(\varepsilon_2^*)_\beta = st\cos(\theta/2)(\lambda_1-\lambda_2), \tag{2.6}$$

$$T^{(3)}_{\mu\alpha\beta}\xi_\mu(\varepsilon_1)_\alpha(\varepsilon_2^*)_\beta = st\cos(\theta/2)(1-\lambda_1\lambda_2), \tag{2.7}$$

$$T^{(4)}_{\mu\alpha\beta}\xi_\mu(\varepsilon_1)_\alpha(\varepsilon_2^*)_\beta = -8\frac{s^2u}{t}\cos(\theta/2)\lambda_1\lambda_2, \tag{2.8}$$

where $\theta$ is the angle between the incoming neutrino, which is moving in the $+z$ direction, and the outgoing neutrino, $\lambda_1 = \pm 1$ is the helicity of the incoming photon, and $\lambda_2 = \pm 1$ is the helicity of the outgoing photon. Of these contractions, Eq. (2.6) is antisymmetric under the exchange of $\lambda_1$ and $\lambda_2$. The other three, Eqs. (2.5), (2.7), and (2.8), are symmetric under this exchange. The imposition of time reversal invariance, which implies the symmetry of the amplitude under the exchange of $\lambda_1$ and $\lambda_2$, means that the T-violating part of the helicity basis, Eq. (2.6), must be excluded.

Using Eqs. (2.1), (2.2), (2.5), (2.7), and (2.8), the helicity amplitudes $\mathcal{A}_{\lambda_1\lambda_2}(s,t,u)$ can be written as

$$\mathcal{A}_{++}(s,t,u) = 2s\cos(\theta/2)\left[2u\mathcal{M}_1(s,t,u) - 4\frac{su}{t}\mathcal{M}_4(s,t,u)\right], \tag{2.9}$$

$$\mathcal{A}_{--}(s,t,u) = 2s\cos(\theta/2)\left[-2s\mathcal{M}_1(s,t,u) - 4\frac{su}{t}\mathcal{M}_4(s,t,u)\right], \tag{2.10}$$

$$\mathcal{A}_{+-}(s,t,u) = 2s\cos(\theta/2)\left[(s-u)\mathcal{M}_1(s,t,u) + t\mathcal{M}_3(s,t,u) + 4\frac{su}{t}\mathcal{M}_4(s,t,u)\right], \tag{2.11}$$

$$\mathcal{A}_{-+}(s,t,u) = \mathcal{A}_{+-}(s,t,u), \tag{2.12}$$

where $t = -\frac{1}{2}s(1-z)$, $u = -\frac{1}{2}s(1+z)$, $z = \cos\theta$, and we have assumed time reversal symmetry and, therefore, omitted $\mathcal{M}_2(s,t,u)$. Notice that Eq. (2.12) is the result of T-invariance, not Bose symmetry.

To include the requirements of Bose symmetry, Eqs. (2.3) and (2.4), and also to exhibit the conservation of angular momentum in the expressions for the helicity amplitudes, Eqs. (2.9)–(2.11), we define the following two independent scalar functions:

$$\mathcal{F}(s,t,u) = 4\mathcal{M}_1(s,t,u) - 8\frac{s}{t}\mathcal{M}_4(s,t,u), \tag{2.13}$$

$$\mathcal{G}(s,t,u) = \mathcal{M}_3(s,t,u) - 2\frac{u}{t}\mathcal{M}_1(s,t,u) + 4\frac{su}{t^2}\mathcal{M}_4(s,t,u). \tag{2.14}$$

The interchange of $s$ and $u$ in Eqs. (2.13) and (2.14), together with the Bose symmetry requirements of Eqs. (2.3) and (2.4), result in the following relations:

$$\mathcal{F}(u,t,s) = 4\mathcal{M}_1(s,t,u) + 8\frac{u}{t}\mathcal{M}_4(s,t,u), \tag{2.15}$$

$$\mathcal{G}(u,t,s) = -\mathcal{M}_3(s,t,u) - 2\frac{s}{t}\mathcal{M}_1(s,t,u) - 4\frac{su}{t^2}\mathcal{M}_4(s,t,u). \tag{2.16}$$

Using Eqs. (2.13)–(2.16) in Eqs. (2.9)–(2.11) results in the following general expressions for the helicity amplitudes:

$$\mathcal{A}_{++}(s,t,u) = su\cos(\theta/2)\mathcal{F}(s,t,u), \tag{2.17}$$

$$\mathcal{A}_{--}(s,t,u) = -s^2\cos(\theta/2)\mathcal{F}(u,t,s), \tag{2.18}$$

$$\mathcal{A}_{+-}(s,t,u) = st\cos(\theta/2)[\mathcal{G}(s,t,u) - \mathcal{G}(u,t,s)]. \tag{2.19}$$

In order to ensure the conservation of angular momentum in Eqs. (2.17)–(2.19), it is necessary to require that the functions $\mathcal{F}(s,t,u)$, $\mathcal{F}(u,t,s)$, and $[\mathcal{G}(s,t,u) - \mathcal{G}(u,t,s)]$ be nonsingular in the limit $u \to 0$ (backward scattering). In addition, the function $[\mathcal{G}(s,t,u) - \mathcal{G}(u,t,s)]$ must also be nonsingular in the limit $t \to 0$ (forward scattering).

From Eqs. (2.17)–(2.19), it is clear that the interchange of $s$ and $u$, results in the following relation:

$$\mathcal{A}_{\lambda_1\lambda_2}(s,t,u) = \mathcal{A}_{-\lambda_1-\lambda_2}(u,t,s), \tag{2.20}$$

where, under this interchange, the factor $s\cos(\theta/2) = s\sqrt{-u/s}$ becomes $u\sqrt{-s/u} = -s\sqrt{-u/s} = -s\cos(\theta/2)$.

We can use Eq. (2.20) as a check of our calculation. To do this, we must express the helicity amplitudes as functions of $s$ and $u$ such that these functions remain well defined after the interchange $s \leftrightarrow u$. A certain amount of care must be exercised when performing a numerical check of Eq. (2.20), because it is convenient to use the fact that $s > 0$ and $u < 0$ when calculating $\mathcal{A}_{\lambda_1\lambda_2}(s,t,u)$. The interchange of $s$ and $u$ would seem to move the numerical calculation into the region $s < 0$ and $u > 0$ in order to make the comparison. However, no additional calculation is required if one remembers that each of the diagrams of Fig. 1 has a counterpart in which the photons are interchanged. If a particular scalar contribution to one of the direct diagrams is $f(s,u)$ the corresponding crossed diagram will contribute $f(u,s)$. When it is assumed that $s > 0$ and $u < 0$, the result is a function $f_1(s,u)$ for the direct diagram and a different function $f_2(u,s)$ for the crossed diagram. The function $f_1(x,y)$ is not defined when its first variable is negative and its second positive, while $f_2(x,y)$ is not defined when its first variable is positive and

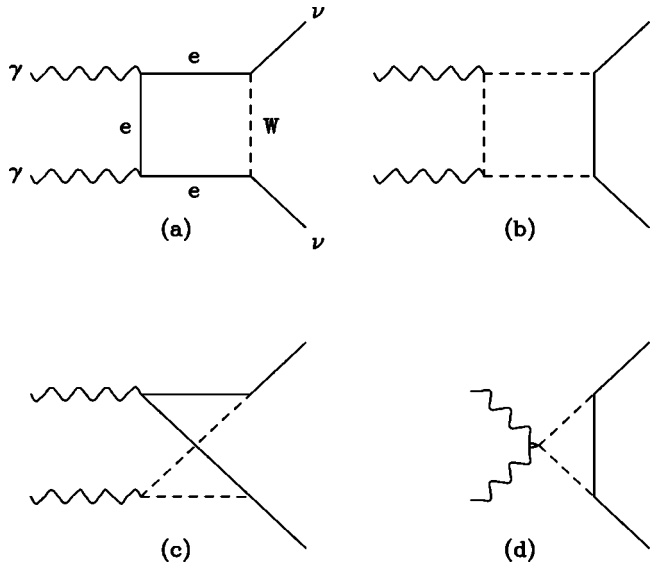


FIG. 1. Diagrams for the process $\gamma\nu_e \to \gamma\nu_e$ are shown. Diagram (d) gives a vanishing contribution. For each of (a), (b), (c) there is also a diagram with the photons interchanged.

its second is negative. Since the $s \leftrightarrow u$ interchange essentially exchanges the direct and crossed contributions, we can use

$$F(s,u) = \theta(s)\,\theta(-u) f_1(s,u) + \theta(-s)\,\theta(u) f_2(s,u) \tag{2.21}$$

for the direct contribution and

$$F(u,s) = \theta(u)\,\theta(-s) f_1(u,s) + \theta(-u)\,\theta(s) f_2(u,s) \tag{2.22}$$

for the crossed contribution. Clearly, $F(s,u)$ and $F(u,s)$ are well defined for both $s>0$, $u<0$ and $s<0$, $u>0$.

### III. DIFFERENTIAL AND TOTAL CROSS SECTIONS

We calculated the diagrams of Fig. 1 in a nonlinear $R_\xi$ gauge such that the coupling between the photon, the $W$ boson and the Goldstone boson vanishes [5,10,11]. Using algebraic manipulation software SCHOONSCHIP [12] and FORM [13], the diagrams were decomposed in terms of scalar $n$-point functions [14,15], and then checked numerically with the FORTRAN codes LOOP [16] and FF [17]. In addition, using Eqs. (2.21) and (2.22), we demonstrated that our numerical calculations for the helicity amplitudes, satisfy Eqs. (2.12) and (2.20). To simplify the calculations, we assumed that $s,t,u \gg m_e^2$. Several of the scalar $n$-point functions depended upon $\ln(m_e)$ or $\ln^2(m_e)$. However, it turns out that every diagram of the Fig. 1 is independent of the $m_e$. Due to the assumption $s,t,u \gg m_e^2$, in general, we do not expect that our results be reliable near the forward and the backward directions, where $t \to 0$ and $u \to 0$, respectively.

To study the degree of reliability, and also as a partial check of our calculated helicity nonflip amplitudes near the forward direction, we use the optical theorem, which relates the imaginary part of the nonflip amplitude for elastic scattering in the forward direction to the total cross section for the process $\gamma\nu \to W^+ e^-$ as

$$-\frac{1}{s}\,\mathrm{Im}\,\mathcal{A}_{\lambda\lambda}(\theta=0) = \sigma_\lambda\,. \tag{3.1}$$

Here, $\lambda$ is the helicity of the photon, and $\sigma_\lambda$ represents the total cross section for a photon of given helicity $\lambda$, after summation over the helicities of the $W$ boson and the electron. Our explicit calculation gives

$$\sigma_+ = 2\sqrt{2} G_F \alpha \left[ \frac{\sqrt{\lambda(s,m_e^2,m_W^2)}}{s} \left(1+\frac{m_W^2}{s}\right)\left(1+2\frac{m_W^2}{s}\right) + \frac{m_W^6}{s^3} l(s,m_W^2,m_e^2) - \frac{m_W^2}{s}\left(1-\frac{m_W^4}{s^2}\right) l(s,m_e^2,m_W^2) \right], \tag{3.2}$$

$$\sigma_- = 2\sqrt{2} G_F \alpha \left[ \frac{\sqrt{\lambda(s,m_e^2,m_W^2)}}{s} \left(1-\frac{m_W^2}{s}\right)\left(1-2\frac{m_W^2}{s}\right) + \frac{m_W^2}{s}\left(1-\frac{m_W^2}{s}\right)^2 l(s,m_W^2,m_e^2) + \frac{m_W^2}{s}\left(1-\frac{m_W^2}{s}\right)^2 l(s,m_e^2,m_W^2) \right], \tag{3.3}$$

where

$$\lambda(x,y,z) = x^2+y^2+z^2-2xy-2xz-2yz, \tag{3.4}$$

$$l(x,y,z) = \ln\left(\frac{x-y+z+\sqrt{\lambda(x,y,z)}}{x-y+z-\sqrt{\lambda(x,y,z)}}\right). \tag{3.5}$$

We retain the electron mass in the functions $\lambda(s,m_W^2,m_e^2)$, $l(s,m_W^2,m_e^2)$, and $l(s,m_e^2,m_W^2)$ to ensure that the cross sections vanish at threshold $\sqrt{s} = m_W + m_e$. In the coefficients of these functions, we have dropped powers of $m_e^2/m_W^2$. The spin averaged cross section $(\sigma_+ + \sigma_-)/2$ agrees with the result previously obtained by Seckel [18].

Both cross sections approach the same constant when $\sqrt{s} \gg m_W$. Since $l(s,m_W^2,m_e^2) \sim \ln(m_W^2/m_e^2)$, each cross section contains a $\ln(m_e^2)$ term, which our numerical calculation of $\mathcal{A}_{\lambda\lambda}(s,\theta)$ will not obtain in the forward direction due to the assumption $s,t,u \gg m_e^2$. Nevertheless, we can use the optical theorem to check the high energy behavior of our amplitudes because the $\ln(m_W^2/m_e^2)$ terms in $\sigma_+$ and $\sigma_-$ depend very differently on $m_W^2/s$; $(m_W^2/s)^3$ versus $m_W^2/s$. Indeed, for $\sqrt{s} \gtrsim 200\,\mathrm{GeV}$, and $\lambda = +1$, our calculations for the $-\mathrm{Im}\,\mathcal{A}_{++}(\theta=0)/s$ and $\sigma_+$ are in good agreement with Eq. (3.1), while for $\lambda = -1$, the cross section $\sigma_-$ is almost a factor of two larger than the quantity $-\mathrm{Im}\,\mathcal{A}_{--}(\theta=0)/s$. However, at higher energies, we find an excellent agreement with Eq. (3.1) for both $\lambda = \pm 1$ helicities.

Before leaving the subject of the behavior of the nonflip forward helicity amplitudes, it is worth noting that the exact

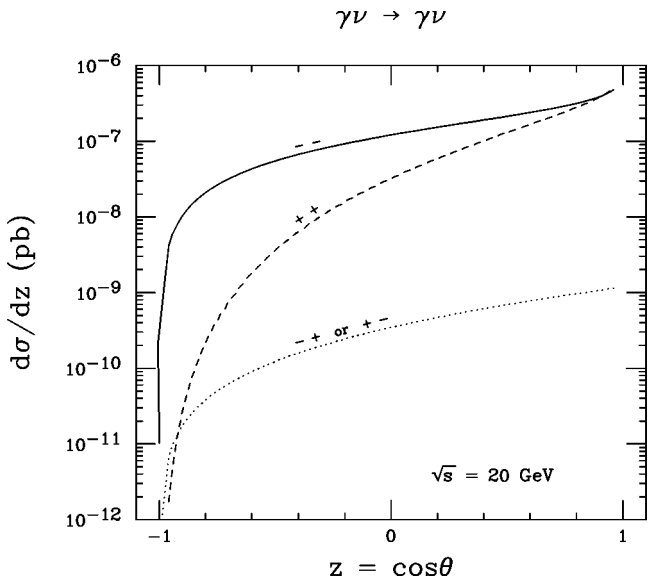


FIG. 2. The helicity dependent differential cross sections for $\gamma\nu\to\gamma\nu$ are shown for $\sqrt{s}=20\,\mathrm{GeV}$. The solid line is $d\sigma_{--}/dz$, the dashed line is $d\sigma_{++}/dz$, and the dotted line is $d\sigma_{+-}/dz = d\sigma_{-+}/dz$.

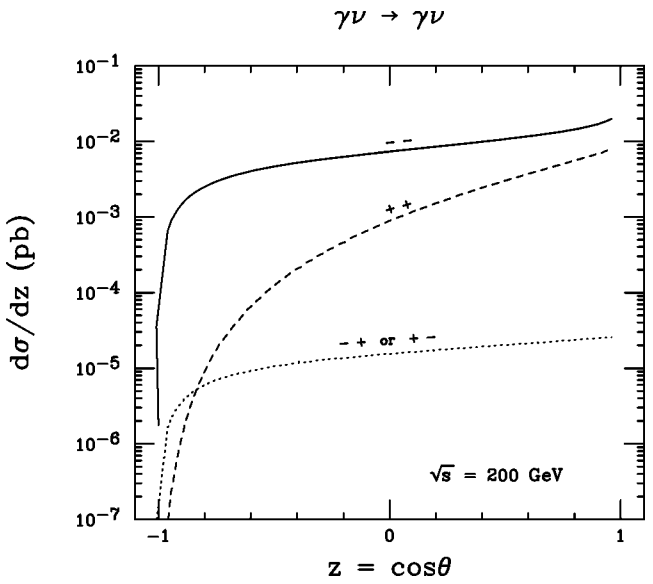


FIG. 3. Same as Fig. 2 with $\sqrt{s}=200\,\mathrm{GeV}$.

value of the forward helicity amplitude $\mathcal{A}_{\lambda\lambda}(s)$ can be obtained using the dispersion relation

$$\mathcal{A}_{\lambda\lambda}(s)=\frac{s^2}{\pi}\int_{(m_W+m_e)^2}^{\infty}\frac{ds'}{s'}\left(\frac{\sigma_\lambda(s')}{s'-s}+\frac{\overline{\sigma}_\lambda(s')}{s'+s}\right), \quad (3.6)$$

where $\overline{\sigma}_\lambda(s)$ is the cross section in the channel $\gamma\overline{\nu}\to W^- e^+$. It is not difficult to show that $\overline{\sigma}_\lambda(s)=\sigma_{-\lambda}(s)$, in which case we have

$$\mathcal{A}_{\lambda\lambda}(s)=\frac{s^2}{\pi}\int_{(m_W+m_e)^2}^{\infty}\frac{ds'}{s'}\left(\frac{\sigma_\lambda(s')}{s'-s}+\frac{\sigma_{-\lambda}(s')}{s'+s}\right). \quad (3.7)$$

This expression obeys the symmetry relation (2.20) specialized to the forward direction $t=0$,

$$\mathcal{A}_{\lambda\lambda}(s)=\mathcal{A}_{-\lambda-\lambda}(-s). \quad (3.8)$$

To leading order in $s$, the dispersion integral can be evaluated and gives

$$A_{++}(s)=A_{--}(s)=\frac{\sqrt{2}G_F\alpha s^2}{\pi m_W^2}\left[\frac{2}{3}\ln\left(\frac{m_W^2}{m_e^2}\right)+\frac{1}{2}\right], \quad (3.9)$$

in agreement with the low energy result of Ref. [5]. Details will be presented elsewhere.

In Figs. 2 and 3 we show the differential cross sections for elastic scattering using

$$\frac{d\sigma_{\lambda_1\lambda_2}}{dz}=\frac{1}{32\pi s}|\mathcal{A}_{\lambda_1\lambda_2}|^2, \quad (3.10)$$

where, $\lambda_1$ and $\lambda_2$ are the helicities of the incoming and outgoing photons, respectively. Figures 2 and 3 illustrate the identity of the amplitudes $\mathcal{A}_{+-}$ and $\mathcal{A}_{-+}$, as required by Eq. (2.12). They also show the vanishing of the amplitudes for backward scattering, $\theta=\pi$. However, they do not exhibit the vanishing of the $\mathcal{A}_{+-}$ or $\mathcal{A}_{-+}$ in the forward direction, $\theta=0$. As we stated earlier we do not, in general, expect our results be reliable near the forward $(t\to 0)$ and backward $(u\to 0)$ directions on a scale $\sim m_e^2$. In our calculations, we have, for instance, replaced factors such as $t/(t-m_e^2)$ with 1. This situation is analogous to that encountered when calculating the amplitudes for quark+gluon→quark+photon [19], where the existence of the kinematic zeros proportional to $t$ in the forward direction is obscured by the assumption that the quarks are massless. A similar phenomenon occurs when calculating photon-photon scattering in massless QED. There certain amplitudes involving spacelike longitudinal photons fail vanish as $k^2\to 0$ because factors such as $k^2/(k^2+m^2)$ become 1 in the limit $m^2\to 0$ [20].

The total cross sections, for helicities $\lambda_1$ and $\lambda_2$, are given by

$$\sigma_{\lambda_1\lambda_2}=\frac{1}{32\pi s}\int_{-1}^{1}dz|\mathcal{A}_{\lambda_1\lambda_2}|^2, \quad (3.11)$$

and are plotted in Fig. 4. Shown in dots is the cross section for helicity flip scattering, which can be seen to be much smaller than the cross sections for the helicity nonflip scattering. This feature seems not to be a consequence of any symmetry, but it is reminiscent of the low energy case $(\sqrt{s}\ll m_e)$, where the helicity flip amplitudes vanish [5]. In Fig. 5, we show the total cross section for an unpolarized initial photon

$$\sigma_{\gamma\nu\to\gamma\nu}=\frac{1}{2}(\sigma_{--}+\sigma_{++}+\sigma_{+-}+\sigma_{-+}). \quad (3.12)$$

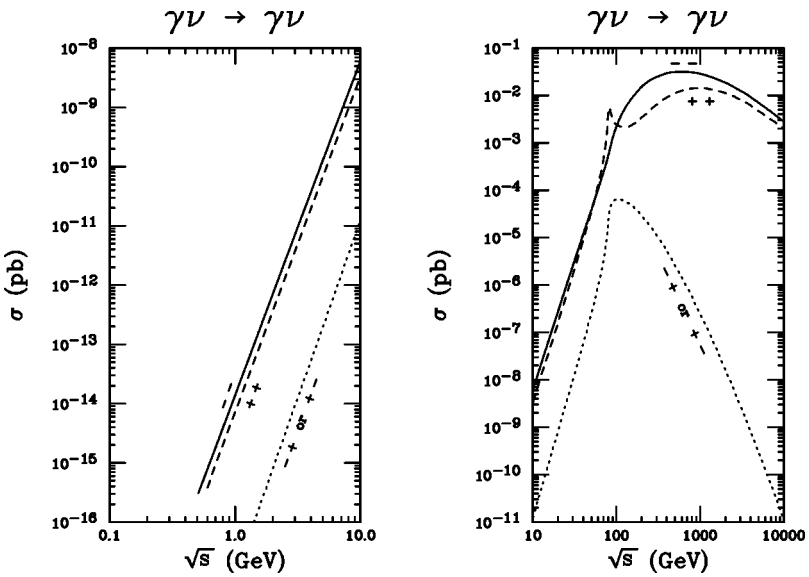


FIG. 4. The helicity dependent total cross sections for $\gamma\nu\to\gamma\nu$ are shown. The solid line is $\sigma_{--}$, the dashed line is $\sigma_{++}$, and the dotted line is $\sigma_{+-}=\sigma_{-+}$.

This figure illustrates the roughly $s^3$ behavior of the total cross section to near the threshold for the $W$-boson production. A fit to the points in Fig. 5, for $m_e \ll \omega \ll m_W$, yields

$$\sigma_{\gamma\nu\to\gamma\nu} = 6.7\times 10^{-33}\left(\frac{\omega}{m_e}\right)^6 \text{ pb}, \tag{3.13}$$

where $\omega=\sqrt{s}/2$ is the energy of a photon (or a neutrino). In the Ref. [21], it is shown that the cross section for the process $\gamma\nu\to\gamma\gamma\nu$, in the range of energies $m_e \ll \omega \ll m_W$, can be written as

$$\sigma_{\gamma\nu\to\gamma\gamma\nu} = 1.74\times 10^{-16}\left(\frac{\omega}{m_e}\right)^2 \text{ pb}. \tag{3.14}$$

Comparison of Eq. (3.13) with Eq. (3.14) shows that the two cross sections are equal for $\omega=1.27\times 10^4 m_e$ or $\sqrt{s}=13\,\text{GeV}$. Therefore, at sufficiently high energies, the process $\gamma\nu\to\gamma\nu$ dominates the process $\gamma\nu\to\gamma\gamma\nu$.

## IV. DISCUSSION AND CONCLUSIONS

As shown above, the cross section for elastic scattering is larger than the cross section for the inelastic scattering when $\sqrt{s}\gtrsim 13\,\text{GeV}$. Since the weak interaction violates parity, the final photons in both processes acquire circular polarization. In the case of inelastic scattering, it is shown in Refs. [7] and [21] that the circular polarization is of order $20-30\,\%$ for center of mass energies less than $100 m_e$.

To assess the degree of circular polarization of the final photon in the elastic scattering, we define the polarization $P$ as

$$P=\frac{\sigma_{--}+\sigma_{+-}-\sigma_{-+}-\sigma_{++}}{\sigma_{--}+\sigma_{+-}+\sigma_{-+}+\sigma_{++}}, \tag{4.1}$$

or, since $\sigma_{+-}=\sigma_{-+}\ll\sigma_{--}$,

$$P\simeq\frac{\sigma_{--}-\sigma_{++}}{\sigma_{--}+\sigma_{++}}. \tag{4.2}$$

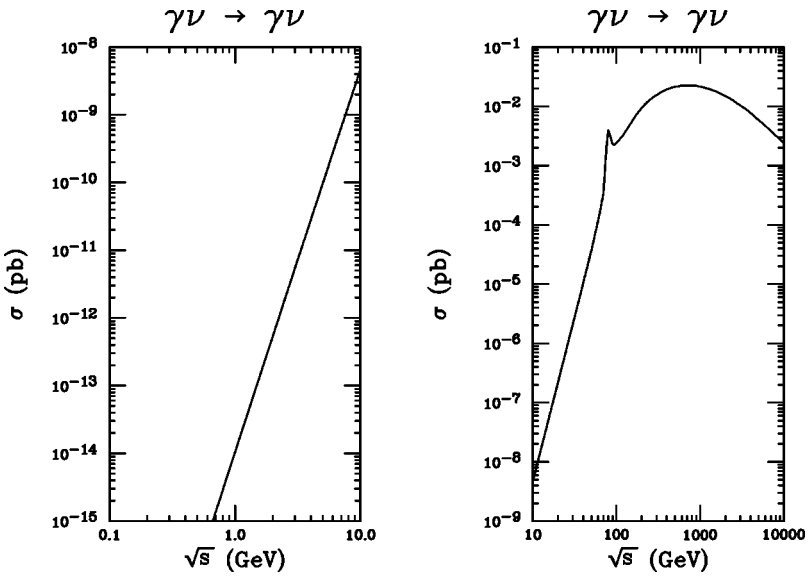


FIG. 5. The total cross section $\sigma_{\gamma\nu\to\gamma\nu}$ for unpolarized photons is shown.

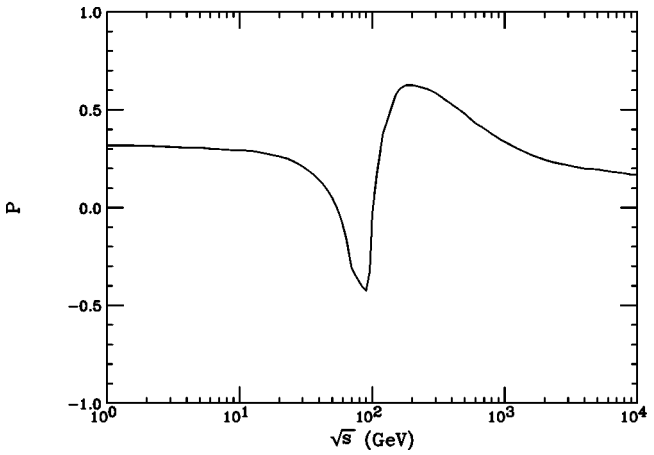


FIG. 6. The circular polarization $P$ of the final photon in the process $\gamma\nu\rightarrow\gamma\nu$, as defined in Eq. (4.1), is shown. For $\sqrt{s}\ll 2m_e$ [5], $P$ is $\frac{1}{3}$.

In Fig. 6, we have plotted the polarization $P$ as a function of the center-of-mass energy $\sqrt{s}$. As is clear from this graph, for a wide range of energies above 1 GeV, the polarization is of order 20−30 %, while for energies around 200 GeV it can reach over 60%. To find $P$ for center-of-mass energies $\sqrt{s}\ll 2m_e$, we can use the helicity amplitudes in Eq. (4) of Ref. [5], to obtain $P=\frac{1}{3}$.

The angular dependence of the the final photon's polarization can be obtained from $P(z)$ defined as

$$P(z)=\frac{d\sigma_{--}/dz+d\sigma_{+-}/dz-d\sigma_{-+}/dz-d\sigma_{++}/dz}{d\sigma_{--}/dz+d\sigma_{+-}/dz+d\sigma_{-+}/dz+d\sigma_{++}/dz} \tag{4.3}$$

or, since $d\sigma_{+-}/dz=d\sigma_{-+}/dz$,

$$P(z)=\frac{d\sigma_{--}/dz-d\sigma_{++}/dz}{d\sigma_{--}/dz+2d\sigma_{+-}/dz+d\sigma_{++}/dz}. \tag{4.4}$$

The polarization $P(z)$ is plotted in Fig. 7 as a function of $z=\cos\theta$. In this figure, the solid line is effectively unchanged for the range of center-of-mass energies $1\,\mathrm{GeV}\lesssim\sqrt{s}\lesssim 30\,\mathrm{GeV}$. The dashed curve shows that the forward amplitudes $\mathcal{A}_{++}(s)$ and $\mathcal{A}_{--}(s)$ are not equal above the threshold for $W$ production. This is consistent with the dispersion relation (3.7). Also included in this figure is the polarization for the case $\sqrt{s}\ll 2m_e$, which is based on Eq. (5) of Ref. [5] $[P(z)=-\mathcal{P}(\theta)]$.

It is worth noting that both the $s^3$ behavior of the elastic cross section and the angular dependence of $P(z)$ obtained in the low energy limit [5] persist to energies of order $m_W$. This means that a low energy effective interaction of the form [22]

$$\mathcal{L}_{\mathrm{eff}}=\frac{1}{8\pi}\frac{g^2\alpha}{m_W^4}AT^{\nu}_{\lambda\rho}T^{\gamma}_{\lambda\rho}, \tag{4.5}$$

where $T^{\nu}_{\lambda\rho}$ and $T^{\gamma}_{\lambda\rho}$ are the symmetrical energy-momentum tensors of the neutrino and the photon, gives an accurate description of elastic scattering to quite high energies.

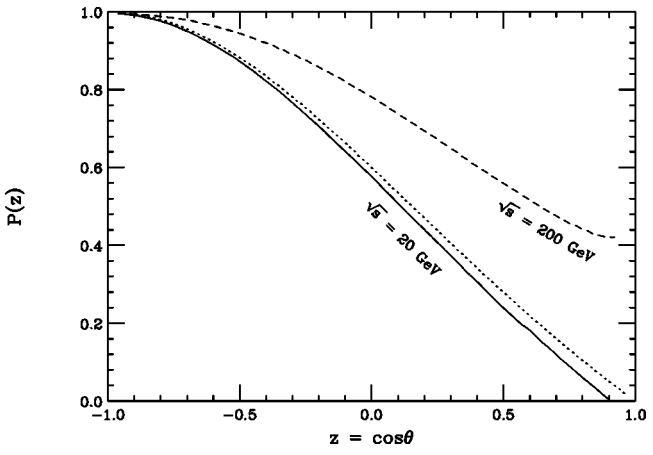


FIG. 7. The circular polarization $P(z)$ of the final photon in the process $\gamma\nu\rightarrow\gamma\nu$, as defined in Eq. (4.4), is shown. The solid and the dashed lines are polarization for the center of mass energies of 20 and 200 GeV, respectively, while the dotted line is for $\sqrt{s}\ll 2m_e$, which is taken from Ref. [5].

Finally, to investigate the importance of the reaction $\gamma\nu\rightarrow\gamma\nu$ in cosmology, we define $\sigma_\nu$ by

$$\sigma_\nu=\frac{1}{n_\nu ct}, \tag{4.6}$$

where $n_\nu$ is the neutrino number density (number of neutrinos per unit volume), $c$ is the speed of light, and $t$ is the expansion time of the universe. Taking $n_\nu=56\,\mathrm{cm}^{-3}$ and $t=15\times10^9$ yr, we find the present value of $\sigma_\nu$ to be

$$\sigma_\nu=1.26\times10^6\ \mathrm{pb}. \tag{4.7}$$

The mean number of collisions between a photon and relic neutrinos [23] is of order $\sigma_{\gamma\nu\rightarrow\gamma\nu}/\sigma_\nu$. From Fig. 5 and Eq. (4.7) we find that, regardless of the center-of-mass energy $\sigma_{\gamma\nu\rightarrow\gamma\nu}/\sigma_\nu\lesssim10^{-7}$. Therefore, the process $\gamma\nu\rightarrow\gamma\nu$ effectively ceased to occur early in the evolution of the universe.

To estimate the time (or the temperature) at which the decoupling of photons and neutrinos in the process $\gamma\nu\rightarrow\gamma\nu$ took place, we must determine when the value of the ratio $\sigma_{\gamma\nu\rightarrow\gamma\nu}/\sigma_\nu$ is of order 1,

$$\sigma_{\gamma\nu\rightarrow\gamma\nu}/\sigma_\nu\sim1. \tag{4.8}$$

To do this, consider the product $\sigma(p_\gamma,p_\nu)v_{\gamma\nu}$, where $\sigma(p_\gamma,p_\nu)$ is the cross section for the scattering of a photon of momentum $\vec{p}_\gamma$ with a neutrino of momentum $\vec{p}_\nu$, and $v_{\gamma\nu}$ is the magnitude of their relative velocity. We define the average value of this product by

$$\langle\sigma(p_\gamma,p_\nu)v_{\gamma\nu}\rangle=\frac{\int dn_\gamma dn_\nu\sigma(p_\gamma,p_\nu)v_{\gamma\nu}}{\int dn_\gamma,dn_\nu}, \tag{4.9}$$

where

$$dn_\gamma=\frac{1}{(2\pi)^3}\frac{2d^3p_\gamma}{e^{E_\gamma/T}-1}, \tag{4.10}$$

$$dn_\nu = \frac{1}{(2\pi)^3}\frac{d^3p_\nu}{e^{E_\nu/T}+1}. \tag{4.11}$$

Here, $E_\gamma$ and $E_\nu$ are the energies of the photon and neutrino, respectively, and the factor 2 in Eq. (4.10) is due to the number of helicity states of the photon. After performing the integration in the denominator of Eq. (4.9), we obtain

$$\langle \sigma(p_\gamma,p_\nu)v_{\gamma\nu}\rangle = \frac{1}{n_\gamma n_\nu}\int dn_\gamma dn_\nu \sigma(p_\gamma,p_\nu)v_{\gamma\nu}, \tag{4.12}$$

where $n_\gamma$ and $n_\nu$, the number densities for the photons and neutrinos, respectively, are

$$n_\gamma = \frac{1}{(2\pi)^3}\int \frac{2d^3p_\gamma}{e^{E_\gamma/T}-1} = \frac{2\zeta(3)T^3}{\pi^2}, \tag{4.13}$$

$$n_\nu = \frac{1}{(2\pi)^3}\int \frac{d^3p_\nu}{e^{E_\nu/T}+1} = \frac{3\zeta(3)T^3}{4\pi^2}. \tag{4.14}$$

Using the invariance of $\sigma(p_\gamma,p_\nu)v_{\gamma\nu}E_\gamma E_\nu$, the product $\sigma(p_\gamma,p_\nu)v_{\gamma\nu}$ can be expressed in terms of the cross section $\sigma_{\text{c.m.}}$ in the center-of-mass as

$$\sigma(p_\gamma,p_\nu)v_{\gamma\nu} = \sigma_{\text{c.m.}}\frac{2E_{\text{c.m.}}^2}{E_\gamma E_\nu}, \tag{4.15}$$

where $\sigma_{\text{c.m.}}=\sigma_{\gamma\nu\to\gamma\nu}$ is given by Eq. (3.13) with $\omega=E_{\text{c.m.}}$. The center-of-mass energy $E_{\text{c.m.}}$ for a photon (or a neutrino) in terms of $E_\gamma$, $E_\nu$, and $\theta_{\gamma\nu}$, the angle between $\vec{p}_\gamma$ and $\vec{p}_\nu$, is

$$E_{\text{c.m.}} = \sqrt{E_\gamma E_\nu}\sin(\theta_{\gamma\nu}/2). \tag{4.16}$$

Therefore, Eqs. (3.13), (4.15), and (4.16) give

$$\sigma(p_\gamma,p_\nu)v_{\gamma\nu} = 6.7\times10^{-33}\frac{2E_\gamma^3E_\nu^3}{m_e^6}\sin^8(\theta_{\gamma\nu}/2)\,\text{pb}. \tag{4.17}$$

Using this result in Eq. (4.12) and performing the integration, we find

$$\langle \sigma(p_\gamma,p_\nu)v_{\gamma\nu}\rangle = 6.7\times10^{-33}\frac{124}{59535}\frac{\pi^{12}}{[\zeta(3)]^2}\frac{T^6}{m_e^6}\,\text{pb}. \tag{4.18}$$

The average number of collisions that a photon makes with neutrinos through the process $\gamma\nu\to\gamma\nu$ during the time $t$ is

$$\mathcal{N}_\gamma = \langle \sigma(p_\gamma,p_\nu)v_{\gamma\nu}\rangle n_\nu t. \tag{4.19}$$

Similarly, the average number of collisions that a neutrino makes with photons through the process $\gamma\nu\to\gamma\nu$ during the time $t$ is

$$\mathcal{N}_\nu = \langle \sigma(p_\gamma,p_\nu)v_{\gamma\nu}\rangle n_\gamma t. \tag{4.20}$$

For the duration time, we take an expansion time, which is given by [24]

$$t = \frac{2\times10^{20}}{T^2}\,\text{s}, \tag{4.21}$$

where $T$ is the temperature in Kelvin. To estimate the temperature at which the thermal decoupling of the photons and neutrinos took place, we use the criterion

$$\max[\mathcal{N}_\gamma,\mathcal{N}_\nu]\sim 1. \tag{4.22}$$

It is clear from Eqs. (4.13) and (4.14) that $n_\gamma > n_\nu$, and from Eqs. (4.19) and (4.20) that $\mathcal{N}_\gamma < \mathcal{N}_\nu$. Therefore, Eq. (4.22) gives

$$\mathcal{N}_\nu \sim 1. \tag{4.23}$$

Using Eqs. (4.21), (4.13), (4.18), and (4.20), we find

$$\mathcal{N}_\nu = 2.5\times10^{-92}T^7. \tag{4.24}$$

Thus, from Eq. (4.23) we find the decoupling temperature $T\sim 1.2\times10^{13}$ K, or $T\sim 1$ GeV. This translates into an expansion time of about $1.4\times10^{-6}$ s. The temperature $T\sim 1$ GeV corresponds to a center-of-mass energy $\sqrt{s}\sim 2$ GeV, which is well within the range of validity of Eq. (3.13).

## ACKNOWLEDGMENTS

We wish to thank Duane Dicus for numerous helpful discussions. One of us (A.A.) wishes to thank the Department of Physics and Astronomy at Michigan State University for its hospitality and computer resources. This work was supported in part by the National Science Foundation under Grants No. PHY-9802439 and PHY-0070443 and by Confinziamento MURST-PRIN.

[1] H.-Y. Chiu and P. Morrison, Phys. Rev. Lett. **5**, 573 (1960).
[2] M. J. Levine, Nuovo Cimento A **48**, 67 (1967).
[3] L. F. Landovitz and W. M. Schreiber, Nuovo Cimento Soc. Ital. Fis., A **2A**, 359 (1971).
[4] V. K. Cung and M. Yoshimura, Nuovo Cimento Soc. Ital. Fis., A **29A**, 557 (1975).
[5] D. A. Dicus and W. W. Repko, Phys. Rev. D **48**, 5106 (1993).
[6] J. Liu, Phys. Rev. D **44**, 2879 (1991).
[7] D. A. Dicus and W. W. Repko, Phys. Rev. Lett. **79**, 569 (1997).
[8] A. Abbasabadi, A. Devoto, D. A. Dicus, and W. W. Repko, Phys. Rev. D **59**, 013012 (1999).
[9] For a related decomposition in the case $\nu'\to\nu\gamma\gamma$, see J. F. Nieves, Phys. Rev. D **28**, 1664 (1983).
[10] M. B. Gavela, G. Girardi, C. Malleville, and P. Sorba, Nucl. Phys. **B193**, 257 (1981); M. Bace and N. D. Hari Dass, Ann. Phys. (N.Y.) **94**, 349 (1975).
[11] J. F. Nieves, P. B. Pal, and D. G. Unger, Phys. Rev. D **28**, 908

(1983).
[12] M. J. G. Veltman, ''SCHOONSCHIP A Program for Symbol Handling,'' University of Michigan report, 1984.
[13] J. A. M. Vermaseren, ''The Symbolic Manipulation Program FORM,'' Report No. KEK-TH-326, 1992.
[14] G. Passarino and M. Veltman, Nucl. Phys. **B160**, 151 (1979).
[15] G. 't Hooft and M. Veltman, Nucl. Phys. **B153**, 365 (1979).
[16] C. Kao and D. A. Dicus, LOOP, a FORTRAN program for evaluating loop integrals based on the results in Refs. [14] and [15].
[17] G. J. van Oldenborgh, Report No. NIKHEF-H/90-15, 1990.
[18] D. Seckel, Phys. Rev. Lett. **80**, 900 (1998).
[19] A. Devoto, J. Pumplin, W. Repko, and G. L. Kane, Phys. Rev. Lett. **43**, 1062 (1979).
[20] A. S. Gorsky, B. L. Ioffe, and A. Yu. Khodjamirian, Phys. Lett. B **227**, 474 (1989).
[21] D. A. Dicus, C. Kao, and W. W. Repko, Phys. Rev. D **59**, 013005 (1998).
[22] D. A. Dicus, K. Kovner, and W. W. Repko, Phys. Rev. D **62**, 053013 (2000).
[23] P. J. E. Peebles, *Principles of Physical Cosmology* (Princeton University Press, Princeton, NJ, 1993), Chap. 6.
[24] Strickly speaking, the coefficient 2 in this equation should be replaced by a factor less than 1, since the temperature at which we are interested is of the order $10^{13}$ K. For a discussion see S. Weinberg, *Gravitation and Cosmology* (Wiley, New York, 1972), Chap. 15.